A Multisensor Evaluation of the Asymmetric Convective Model, Version 2 in Eastern Texas

by
Jenna Sue Kolling

A thesis submitted to the faculty of the University of North Carolina at Chapel Hill in partial fulfillment of the requirements for the degree of Master of Science in the Environmental Sciences and Engineering.

Chapel Hill
2011

Approved by:

William Vizuete, Advisor

Harvey Jeffries, Reader

Jonathan Pleim, Reader

ABSTRACT
JENNA SUE KOLLING: A Multisensor Evaluation of the Asymmetric Convective Model, Version 2 in Eastern Texas.
(Under the direction of William Vizuete.)

Although there have been a variety of planetary boundary layer (PBL) schemes developed to represent the effects of turbulence in daytime convective conditions, uncertainties correlated with these schemes remain a large source of inaccuracy in meteorology and air quality model simulations. This study evaluates a new combined local and nonlocal closure PBL scheme, the Asymmetric Convective Model, version 2 (ACM2) in eastern Texas against PBL observations taken from ten radar wind profilers, a ground-based lidar, and multiple daytime radiosonde balloon launches. Comparisons are made between these observations and outputs from the Weather Research and Forecasting (WRF) model version 3.1 with the ACM2 PBL scheme option, as well as outputs from the meteorological modeling that is currently being used to develop ozone control strategies in the HGB area. Results show that the WRF-ACM2 combination is much more accurate at representing the spatial and temporal evolution of the PBL in Eastern Texas.

Contents

List of Tables

List of Figures

Chapter 1

Introduction

Among the most important meteorological parameters that influence air quality is the volume of well-mixed air below the free troposphere called the planetary boundary layer (PBL). The PBL interacts directly with the Earth's surface on a time scale of hours, and with a height that is variable in space and time, ranging between hundreds of meters to several kilometers. During the daytime, solar heating of the Earth's surface can generate buoyant turbulent eddies that efficiently mix the air within the PBL. Consequently, particulate matter and gases are diluted at the ground level while a rapidly growing PBL entrains aged pollutants from the free troposphere above. Our ability to accurately predict air quality is limited by a lack of knowledge of the physical influences on PBL structure, making it particularly difficult to model the early morning rise and afternoon decay. These physical influences include turbulence intermittency, horizontal heterogeneity, and rapid time changes (Dabberdt et al., 2004).

An accurate depiction of the diurnal evolution and vertical mixing within the PBL is necessary for realistic air quality simulations (Seaman, 2000; Ku et al., 2001; Zhang et al., 2007). Largely driven by surface heating, the development of the PBL in mesoscale meteorological models relies on realistic simulations of surface fluxes of moisture and heat. Land surface models (LSMs) are used to parameterize these physical processes, while PBL parameterization schemes (PBL schemes, hereafter) simulate the

vertical transport of heat, moisture, momentum, and trace chemical mixing ratios. Although a variety of PBL schemes have been developed to represent the effects of turbulence in convective conditions, uncertainties correlated with these schemes remain a large source of inaccuracy in model simulations. Most existing PBL schemes, namely local and nonlocal closure models, do not consider both small- and large-scale turbulence. In local closure PBL schemes, turbulent fluxes are computed as functions of local gradients, confining vertical mixing to adjacent grid cells. As a result, local closure schemes, including the Mellor-Yamada-Janjic (Janjic, 1990, 1994) cannot realistically simulate convective conditions, which are characterized by large eddies that can sometimes have a size similar to the boundary layer height itself (Brown, 1996). Simple nonlocal closure models, such as Blackadar (1978) and the Asymmetric Convective Model, version 1, (ACM; Pleim and Chang, 1992) represent only large-scale transport driven by convective plumes, neglecting small-scale turbulent mixing. Although the use of non-local methods in models attempting to simulate the PBL has increased, a method that can accurately represent the diurnal PBL must combine both local and nonlocal components of vertical transport.

The recently developed Asymmetric Convective Model Version 2 (ACM2) PBL scheme (Pleim, 2007a) includes an eddy diffusion component in addition to the explicit nonlocal transport of the original ACM. Preliminary testing with controlled, offline experiments showed that ACM2 was able to simulate realistic PBL heights, temperature profiles, and surface heat fluxes. Spatially and temporally limited observational datasets allowed for a preliminary evaluation of ACM2 in the fifth-generation Pennsylvania State University-National Center for Atmospheric Research Mesoscale Model (MM5) (Pleim, 2007b). When compared to two radar wind profilers (RWP) located in Pittsburgh, PA, and Concord, NH, the model tended to simulate the morning rise in the PBL too quickly. The author postulated that this rapid rise was caused by an early

morning warm bias in MM5 rather than a limitation of ACM2. Comparisons were also made against vertical profile measurements taken from radiosondes launched twice a day in Minneapolis, MN and Little Rock, AS. Data from these profiles showed very close comparisons between observed and modeled potential temperature and relative humidity (Pleim, 2007b). Although initial testing of the ACM2 scheme showed good agreement with this limited dataset of observations, a more spatially and temporally diverse set of observations is necessary to further evaluate ACM2 for use in regulatory air quality models.

Southeast Texas, especially the Houston Galveston Brazoria (HGB) eight-hour ozone (O_3) nonattainment area, offers a unique dataset to address some of the open questions remaining in the preliminary analysis. Since the HGB area is in nonattainment of the National Ambient Air Quality Standard (NAAQS) for O_3, considerable resources have been spent on surface and aloft measurements. A variety of instrumented observations were taken during The Second Texas Air Quality Campaign (TexAQS II) (Parrish et al., 2009), which lasted from January 2005 to December 2006, and had an intensive period of operations between August and October 2006, including the TexAQS II Radical Measurement Project (TRAMP) (Lefer and Rappenglück, 2010). These measurements from both the TexAQS II and TRAMP field studies allow for an extensive view of the horizontally and vertically heterogeneous PBL in Eastern Texas and downtown Houston, and provide a rare opportunity to evaluate the new ACM2 PBL scheme.

The HGB area, which is subject to frequent high O_3 episodes due to the interactions between complex coastal meteorology, emissions of ozone precursors, and atmospheric chemistry, is a severe test for a meteorological model. Land and sea breeze circulations and how they interact with larger-scale synoptic systems, such as the typical summertime high pressure over the Gulf of Mexico, have been found to play a crucial role in

the formation of O_3 in Houston (Banta et al., 2005; Darby, 2005; Vizuete et al., 2008). Consequently, Houston's complex meteorology presents a unique challenge for modeling the spatially and temporally diverse PBL height, a critical component for understanding the formation of ozone and other pollutants (Pérez et al., 2006). As a result of this complexity, considerable resources have been spent on the development of meteorological and air quality modeling episodes in support of a State Implementation Plan (SIP) for attaining the NAAQS for O_3. The retrospective modeling used for the current SIP, prepared by the Texas Commission on Environmental Quality (TCEQ, 2010), includes the August-October 2006 TexAQS II period. The availability of this TCEQ meteorological modeling presents a ready comparison for our evaluation of ACM2 against an existing regulatory modeling episode.

The objective of this study is to evaluate the ACM2 PBL scheme for use in regulatory air quality models by leveraging the advanced observational data available in the HGB area. Specifically, we will be evaluating the ACM2 PBL scheme's ability to accurately simulate the morning growth, maximum height, and evening collapse of the PBL while predicting realistic profiles of temperature and humidity. These results will then be compared with those predicted by the meteorological model currently being used to develop O_3 control strategies in the HGB area.

Chapter 2

Methodology

2.1 Model Configuration

This study compares two models used to simulate the meteorology of Eastern Texas between August and October of 2006. One developed by the Environmental Protection Agency for research purposes (EPA-WRF), the other developed by TCEQ for regulatory purposes (TCEQ-MM5). The EPA used the Weather Research and Forecasting (WRF) model version 3.1 (Skamarock et al., 2008) with the ACM2 PBL scheme option (Pleim, 2007a,b). The TCEQ simulation uses the Fifth Generation Meteorological Model (MM5, version 3.7.3) developed jointly by the National Center for Atmospheric Research and Pennsylvania State University (Grell et al., 1994) with the Eta PBL scheme option, which is the Mellor-Yamada scheme as used in the Eta model (Janjic, 1990, 1994). The Eta PBL scheme is a local closure model, determining vertical mixing from predicted turbulent kinetic energy.

In addition to the ACM2 PBL Scheme, EPA-WRF physics options included the Pleim-Xiu land-surface model (PX LSM; Xiu and Pleim, 2001) with the Pleim surface layer scheme (Pleim, 2006), the rapid radiative transfer model for shortwave and longwave radiation (Mlawer et al., 1997), the Kain-Fritsch 2 cumulus parameterization scheme (Kain, 2004), and the Morrison 2-moment microphysics scheme (Morrison and

Gettelman, 2008).

The TCEQ-MM5 physics options include the NOAH land-surface model (Ek et al., 2003), the rapid radiative transfer model, Grell cumulus parameterization, and the simple ice microphysics. In MM5, observed parameters were assimilated during the model run through a process called four-dimensional data assimilation (FDDA). The fine scale 4-km domain was nudged to observational data obtained from radar wind profilers during TexAQS II. To improve the representation of wind fields and other parameters in MM5, the land use characteristics and sea surface temperatures on all domains were updated with high-resolution satellite measurements. Details of the observational nudging are given in Appendix A of the TCEQ report of the Protocol for Eight-Hour Ozone Modeling of the Houston Galveston/Brazoria Area (TCEQ, 2010).

The Meteorology-Chemistry Interface Processor (MCIP; Byun et al., 1999) version 3.5 was used to process the WRF and MM5 outputs by performing horizontal and vertical coordinate transformations and defining gridding parameters (Otte and Pleim, 2010). The MCIP outputs for both models resulted in a 4-km gridded domain centered over Eastern Texas. The episode period is August 13-October 10, 2006, excluding August 23-26 and September 30 due to missing MM5 modeling data.

2.2 Observations

Observational datasets used in this study came from TexAQS II, a major field study conducted in eastern Texas between June 2005 and October 2006, with an emphasis on the Houston O_3 non-attainment region. Meteorological parameters important to air quality were collected via radar wind profilers (RWPs, Knoderer and MacDonald, 2007), radiosondes (Rappenglück et al., 2008), and a ground-based lidar (Flynn, 2006). The RWPs were in operation throughout the entire episode period, while the lidar

was in operation during the entire month of September and multiple radiosondes were launched per day only during high ozone events in September 2006.

2.2.1 Radar Wind Profilers

A vital component of the TexAQS II field study was a network of ten 915-MHz RWPs. As shown in Figure 2.1, the RWPs were scattered throughout Eastern Texas, placed at varying elevations and distances from the coast. After undergoing a rigorous quality control procedure using the Webber-Wuertz algorithm and manual inspection, reflectivity (signal-to-noise ratio) data from the RWPs were used to estimate hourly heights of the daytime convective boundary layer, with occasional missing reports (Knoderer and MacDonald, 2007). The off-shore Brazos site was not used for this study due to a significant amount of missing data.

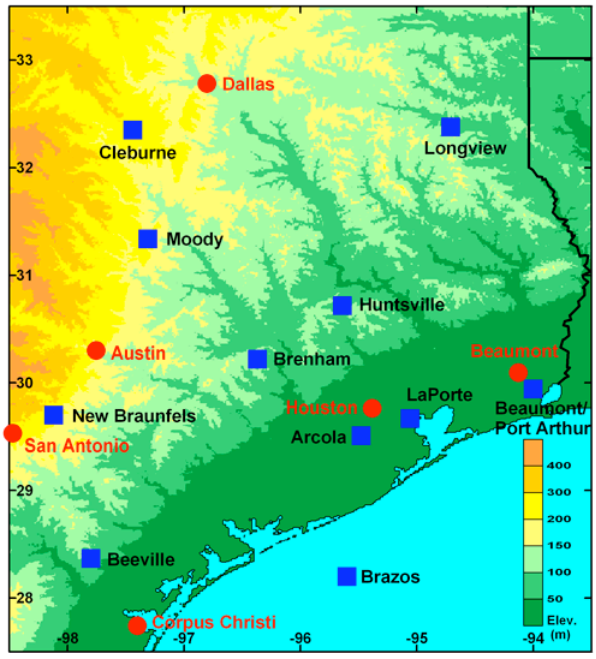

Figure 2.1: Radar wind profiler locations (blue squares) and major cities (red circles) in Eastern Texas during the TexAQS II field campaign. Color shading shows terrain elevation (Wilczak et al., 2009).

2.2.2 Radiosondes

Radiosonde balloons obtain profiles of temperature, pressure, and relative humidity as they ascend through the atmosphere. Normally they are launched twice a day, but for ten days with high O_3 forecasts during September of 2006, five additional balloons were launched from the University of Houston (UH) Moody Tower (Figure 2.2) in downtown Houston, TX. In addition to the radiosonde outputs, vertical profiles were inspected and PBL heights were provided for each balloon launch (Rappenglück et al., 2008).

Figure 2.2: Location of the UH-Moody Tower measurement site (Lefer and Rappenglück, 2010).

2.2.3 Lidar

A ground-based scanning micropulse lidar was deployed on the roof of the UH-Moody Tower (Figure 2.2) during September of 2006 for vertical profiling of the atmosphere. The PBL typically has higher concentrations of aerosols compared to the free troposphere, which means lidar backscatter profiles exhibit a significant negative gradient at the PBL top. Lidar backscatter profiles were visually analyzed to determine PBL depth, except when the lidar was strongly attenuated by low clouds or precipitation (Flynn, 2006).

Chapter 3

Results

For this study, observational data was derived from radar wind profilers, a ground-based lidar, and radiosonde balloon launches. This observational data was used to evaluate meteorological parameters of importance to air quality for direct comparison to outputs from two meteorological models. These include direct comparisons of the WRF model version 3.1 with the ACM2 PBL scheme option, and MM5 version 3.7.3 with the Eta PBL scheme option, which is the meteorological modeling used for the HGB eight-hour O3 standard SIP.

Figure 3.1(a-c) shows the root mean square error (RMSE) between the hourly daytime MM5 and WRF predicted PBL heights and the hourly daytime RWP derived PBL heights for all RWP site locations. Equation 3.1 shows an example of the RMSE calculation for the WRF model at time t.

$$\mathsf{RMSE_{WRF}} = \overline{\sqrt{\mathsf{E_t}((\mathsf{PBL_{WRF,t}} - \mathsf{PBL_{RWP,t}})^2)}} \tag{3.1}$$

where $\mathsf{E_t}$ represents the error at time t, $\mathsf{PBL_{WRF,t}}$ represents the WRF calculated PBL height at time t, and $\mathsf{PBL_{RWP,t}}$ represents the RWP derived PBL height at time t.

RWP locations in Figure 3.1(a-c) are ordered along the x-axis according to location, with the leftmost sites being the furthest inland and the rightmost sites being nearest

to the coast. Figure 3.1a shows the average RMSE of each model between the hours of 8am-11am, representing the models' error in predicting the morning rise of the PBL. MM5 had a larger average RMSE than WRF at all 10 stations, ranging from 20m larger at Longview to 130m larger at Beaumont. Although WRF predicted more realistic PBL heights on average than MM5 during the morning hours, there is a notable increase of about 100m in the WRF RMSE at locations nearer to the coast. Figure 3.1b shows the average RMSE of both models at predicting the daily peak PBL (note the y-scale increase). MM5 had a much larger error than WRF at all 10 stations, ranging from 90m larger at Arcola to 410m at Cleburne, where MM5 had more than double the average RMSE of WRF (735m vs. 325m, respectively). Figure 3.1c shows the RMSE between the hours of 4pm-7pm, representing the models' error in predicting the evening collapse of the PBL. Again, MM5 had a much larger error than WRF, ranging from 130m higher at Beeville to 800m higher at Cleburne.

To further investigate the meteorological models' ability to accurately predict the morning rise, afternoon peak, and evening collapse of the PBL, we looked at the observed temporal evolution of the PBL from the RWPs. The ten RWP stations were divided into three categories according to their location, displayed in Table 3.1.

Table 3.1: Ten RWP stations divided into three categories based on geographic location.

Coastal Plains	Inland	Central Texas
Arcola	Beeville	Cleburne
Beaumont	Brenham	Moody
La Porte	Huntsville	New Braunfels
	Longview	

Figure 3.2(a-c) displays the modeled and observed median PBL for these three regions. The Central Texas location (Figure 3.2a), with drier land use and precipitation patterns, shows the deepest PBL height, with an observed median peak PBL height

(a)

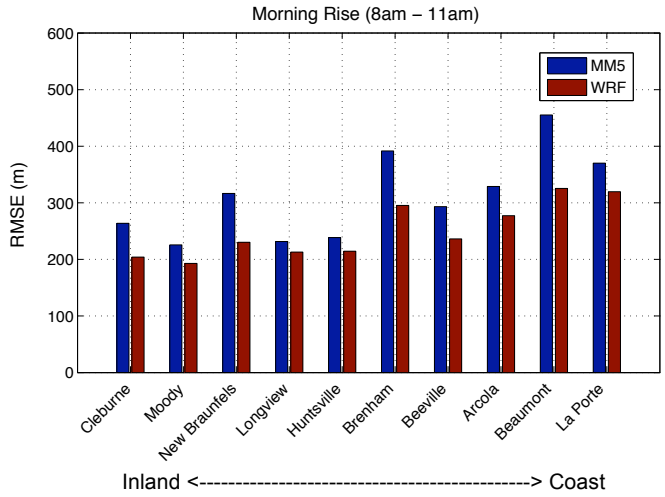

(b)

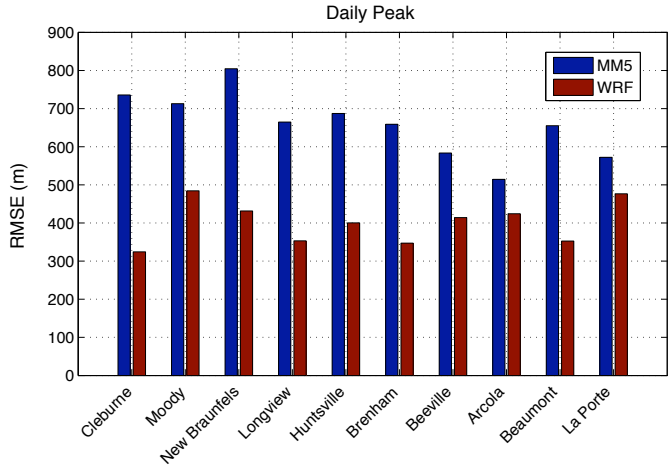

(c)

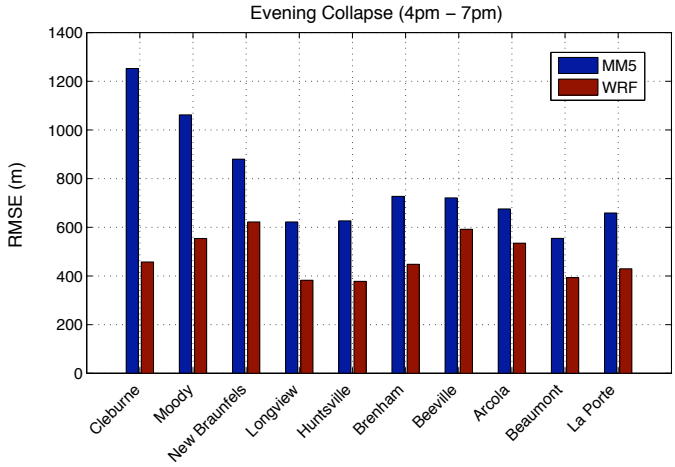

Figure 3.1: Root mean square error for each RWP station location (Ordered furthest inland on the left to nearest to the coast on the right) for the (a) morning rise PBL height (8am-11am), (b) afternoon peak PBL height, and (c) evening collapse PBL height (4pm-7pm).

of over 2000m, which is consistent with the findings of Wilczak et al. (2009) and Hu et al. (2010). Figure 3.2a shows that the MM5 model is severely under-predicting the median height of the PBL in the late morning and afternoon for the Central Texas region by as much as 870m at 1600 CST. The WRF model is more accurate for this time period, with the largest over-prediction of 155m occurring at 1100 CST. Both the WRF and MM5 models predicted an earlier PBL collapse at the Central Texas locations when compared to observations, with MM5 under-predicting by as much as 1350m at 1800 CST, while WRF under-predicted by 275m at the same time. A similar pattern was found at the Inland and Coastal Plains locations (Figures 3.2-b,c), with WRF slightly over-predicting the height of the afternoon median PBL by 260m at 1600 CST in Figure 3.2b, and 240m at 1300 and 1500 CST in Figure 3.2c. MM5 under-predicted the afternoon median PBL height by as much as 700m at 1400 CST at the Inland locations (Figure 3.2b) and 540m at the Coastal Plains locations (Figure 3.2c). At the Inland locations, MM5 collapsed the PBL too early, severely under-predicting the PBL by 865m at 1800 CST (Figure 3.2b), while WRF closely followed the observed PBL collapse with an under-prediction of only 110m at 1800 CST. Similarly, at the Coastal Plains locations, MM5 collapsed the PBL too early, with the largest under-prediction of 760m at 1700 CST (Figure 3.2a), while the largest under-prediction from WRF was 230m at 1700CST.

In a full 3D meteorological model, simulations are affected by many components of model dynamics and physics, such as radiation, cloud cover, land-surface modeling, and large-scale subsidence, thus confounding the evaluation of the PBL scheme (Pleim, 2007a). Surface fluxes of heat and humidity are primarily products of the land-surface model (LSM), and thus surface level temperature and humidity, as well as PBL heights, are influenced much by the LSMs as by the PBL models (Pleim, 2007b). Figure 3.3(a-c) shows the median 2-meter temperature (K) and 2-meter water vapor mixing ratio

(a)

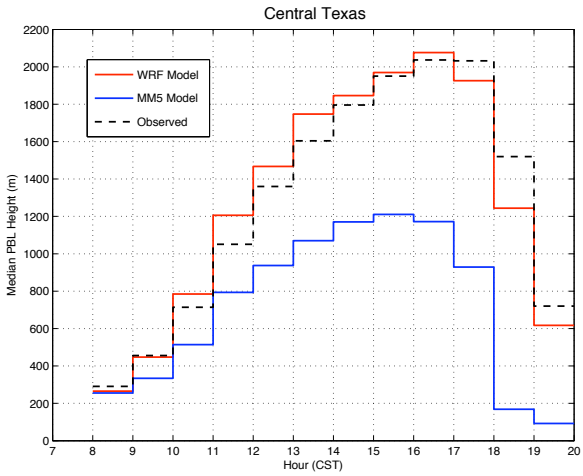

(b)

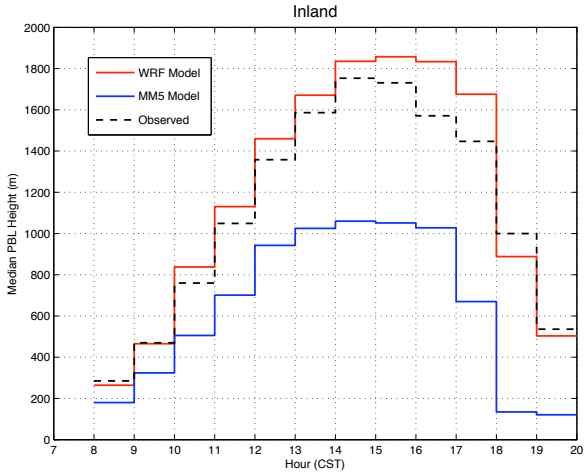

(c)

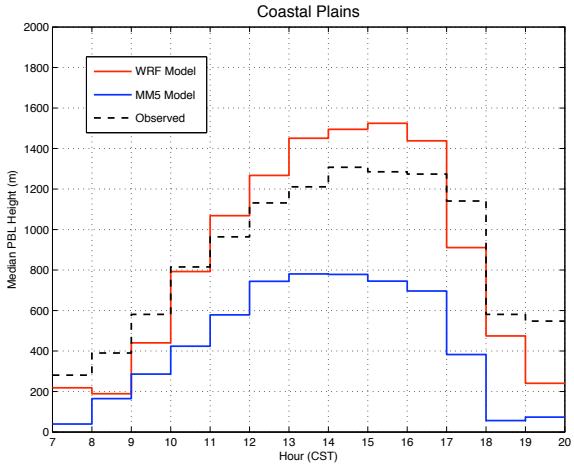

Figure 3.2: Time series of the median hourly PBL height (m) over the entire episode for RWP locations in (a) central Texas, (b) inland, and (c) the coastal plains.

(MR; g/kg) over the entire episode period. Model variables for Figures 3.3 and 3.4 were extracted from the model grid cells corresponding to all ten RWP locations, and then grouped according to regions shown in Table 3.1. Both models have very similar temperature trends during the morning hours for all three regions, but WRF peaks at a 1 K warmer temperature during the afternoon hours for all three regions. WRF is also 2 K warmer during the evening hours, when the PBL is collapsing, at the Central Texas (Figure 3.3a) and Inland (Figure 3.3b) locations. The MM5 model predicted more moisture than WRF for all three regions, with the Coastal Plains having the largest difference in MR of around 2.5 g/kg during the late afternoon hours (Figure 3.3c).

Higher surface temperatures and lower moisture produced by WRF-AMC2 could be a result of surface heat fluxes delivered by the PX LSM and the Pleim surface layer scheme, thus sensible and latent heat fluxes were checked for both WRF-ACM2 and MM5-Eta in Figure 3.4(a-c) for all regions. Lower sensible heat (SH) fluxes and higher latent heat (LH) fluxes would result in lower temperatures at the surface due to the evaporation of moisture, which confines the transfer of heat from the surface to the air. This does not explain the higher temperatures and lower moisture in WRF (from Figure 3.3a) in the Central Texas region (Figure 3.4a), where WRF is shown to have a lower SH flux during the morning and afternoon hours and a higher LH flux throughout the day when compared to the fluxes provided by the NOAH LSM in MM5. Alternatively, SH fluxes in MM5 were lower than WRF during the afternoon and evening hours for the Inland region (Figure 3.4b), and LH fluxes for MM5 were higher than WRF during the afternoon, which could partly explain the lower temperatures and higher moisture in MM5 in Figure 3.3b, although this is unlikely due to the inconsistency of the trend throughout all three regions. Figure 3.4c shows that WRF predicted lower SH fluxes than MM5 during the late morning and early afternoon hours in the Coastal Plains

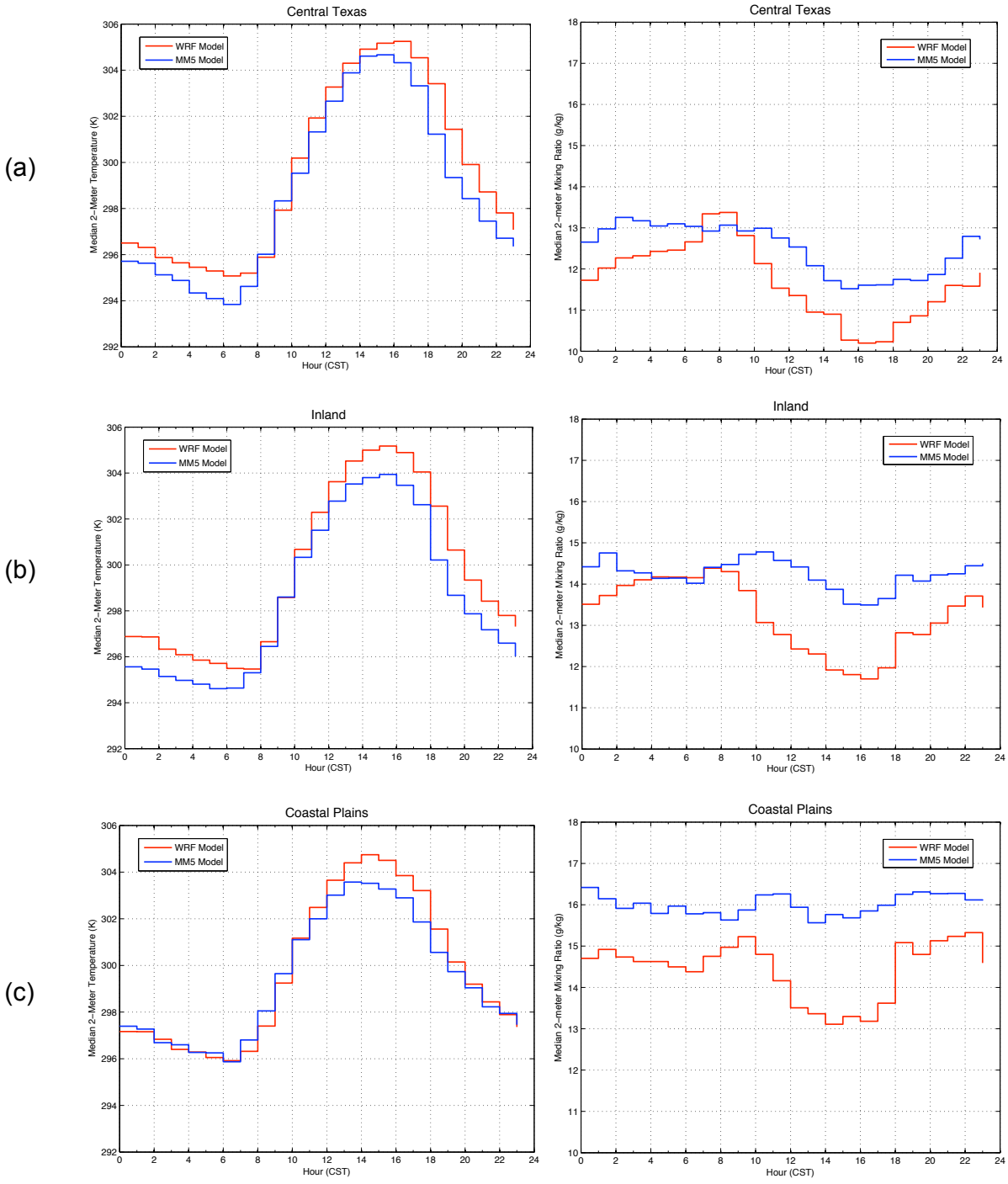

Figure 3.3: Time series of median 2-meter temperature (left) and 2-meter water vapor mixing ratio (right) over the entire episode period for (a) central Texas, (b) Inland, and (c) coastal plains.

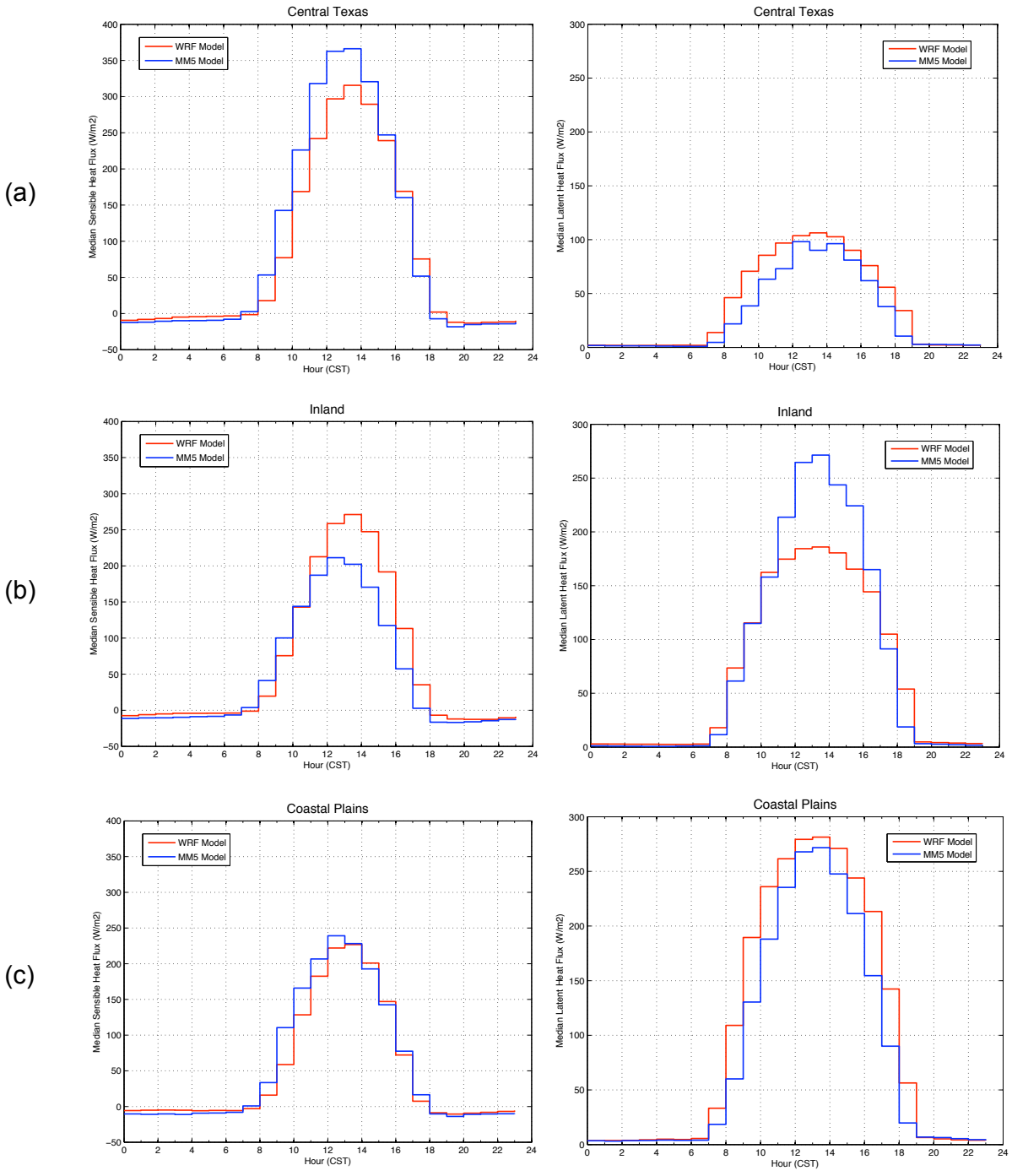

Figure 3.4: Time series of median sensible heat flux (left) and latent heat flux (right) over the entire episode period for (a) central Texas, (b) Inland, and (c) coastal plains.

region, while predicting larger LH fluxes than those predicted by MM5 throughout the day. Again, this trend did not translate into lower surface temperature and higher surface moisture (Figure 3.3c) in WRF as would be expected, further validating that the differences in performance between the models arise directly within the PBL schemes themselves instead of surface layer schemes and surface heat fluxes.

As part of the TexAQS II field campaign, several radiosonde balloons were launched from Moody Tower on the University of Houston main campus, located just west of the Houston Ship Channel (Figure 2.2). Balloons were launched on days with high O_3 forecasts to capture the detailed evolution of the PBL growth (Rappenglück et al., 2008). Simultaneously, a ground-based lidar was capturing vertical profiles of aerosol backscatter above Moody Tower approximately every twenty minutes. Although PBL detection algorithms were applied to the Lidar backscatter data, they were found to be inadequate for the complex atmospheric conditions in Houston due to urban and coastal interactions (Flynn, 2006). Consequently, the lidar profiles were visually inspected to determine PBL heights and have not been fully validated. Although the lidar-derived PBL heights are preliminary, they still serve as a useful comparison to the radiosonde data, which have historically compared well under meteorological conditions favorable for high O_3 events (Nielsen-Gammon et al., 2008b).

Meteorological conditions in the HGB area on September 7, 2006 were favorable for O_3 production due to light winds (5 knots or less), mostly clear skies (except for afternoon boundary-layer cumulus), and high background O_3 concentrations (Nielsen-Gammon et al., 2008a). This particular day was chosen for our study because it is under such low-wind, mostly clear-sky conditions that the PBL scheme would be expected to have the greatest influence on modeled vertical profiles. Figure 3.5 shows a time series of the vertical lidar backscatter profiles on September 7, 2006, with visually estimated PBL heights indicated by the open circles.

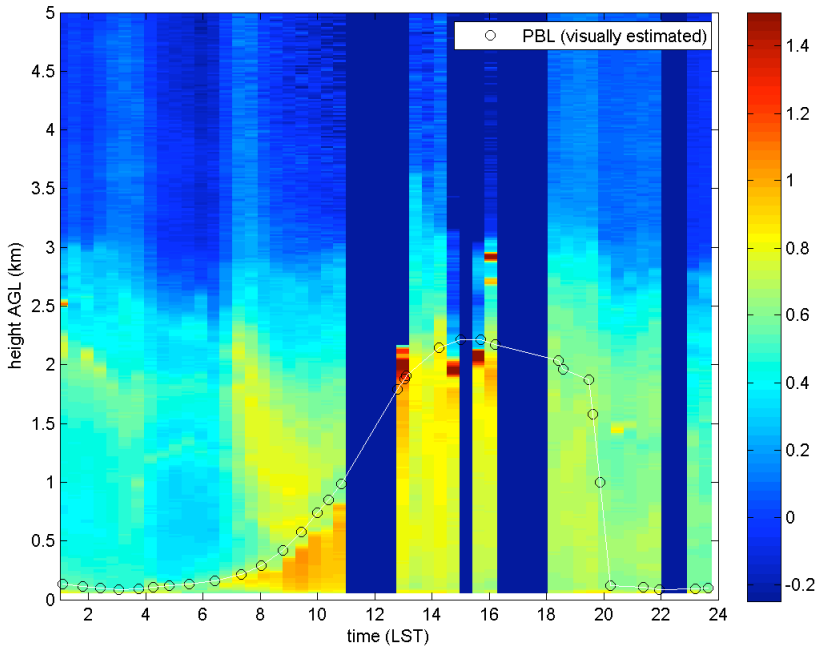

Figure 3.5: Lidar backscatter image from Moody Tower, TX on September 7, 2006. Warm colors indicate higher concentrations of aerosols and open circles indicate visually estimated PBL heights. (Flynn, 2006)

Figure 3.5 is an example of the extreme variability of the PBL depth in the downtown Houston area, with dark blue patches throughout the afternoon and evening indicating the presence of low clouds that suppress PBL growth. Figure 3.6 displays a time series of the visually analyzed lidar PBL heights on September 7, 2006 along with radiosonde-derived and modeled PBL heights. As expected, the lidar-derived PBL heights compare well to those derived from the radiosonde. PBL heights output by the WRF model show a very steep PBL increase of about 1400m between 1000 and 1200 CST, while the lidar-derived PBL heights show a similar increase of 1400m between 1000 and 1300 CST. WRF predicted a 2700m deep afternoon peak PBL, compared to the lidar-derived peak of 2200m and radiosonde-derived peak of 2100m, while MM5 predicted a much more shallow afternoon PBL peak of 1660m. The WRF PBL collapsed 2300m rapidly between 1700 and 1900 CST, while the MM5 model predicts a very gradual

PBL decrease of 1300m between 1500 and 1800 CST. The lidar data was removed between 1600 and 1800 CST due to low clouds in the area, though the lidar-derived PBL heights show a later collapse than both models' predicted of 1900m between 1830 and 2030 CST.

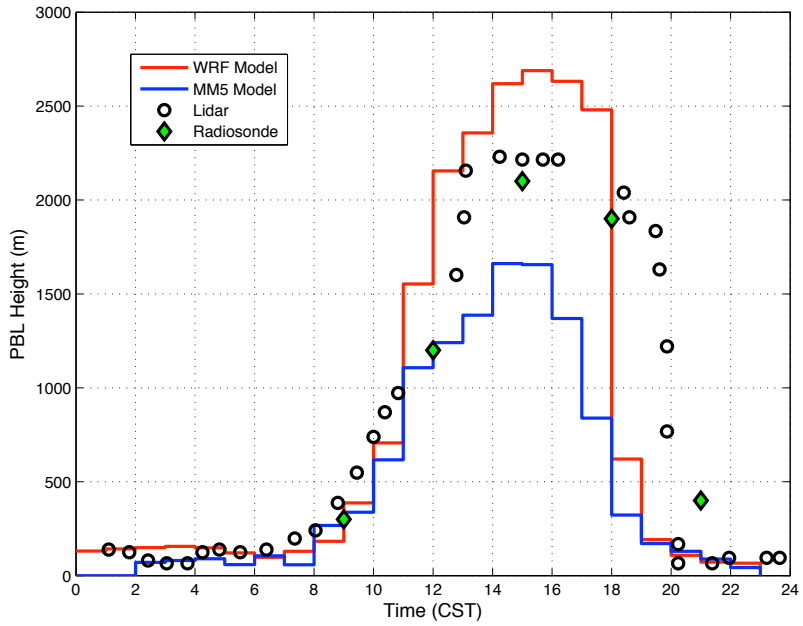

Figure 3.6: Time series of modeled and observed PBL heights on September 7, 2006 at Moody Tower, TX. Open circles indicate visually estimated PBL heights from the lidar backscatter image (Figure 3.5), and green diamonds indicate visually estimated PBL heights from radiosonde profiles (Figure 3.7).

Frequent vertical profiles of potential temperature and humidity through the lowest few kilometers of the atmosphere are the most direct way to test a PBL model. Several radiosonde balloons were launched from Moody Tower, TX on September 7, 2006, five of which were during daytime hours and provide a rare opportunity to evaluate the vertical profiles predicted by WRF-ACM2 and MM5-Eta at multiple times throughout the day. Potential temperature and mixing ratio are both conserved within the PBL, thus finding the point at which a sharp increase in potential temperature and a sharp decrease in mixing ratio (Nielsen-Gammon et al., 2008b) occur signifies the top of

the PBL. Figure 3.7(a-e) displays modeled and observed vertical profiles of potential temperature (left) and mixing ratio (right) at 0900, 1200, 1500, 1800, and 2100 CST. The horizontal green line on each profile represents the height of the PBL as diagnosed from the observed profiles (black dots).

(a)

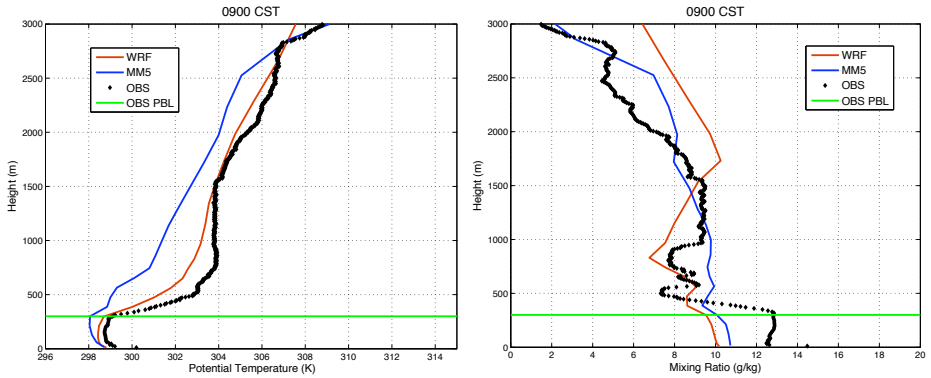

(b)

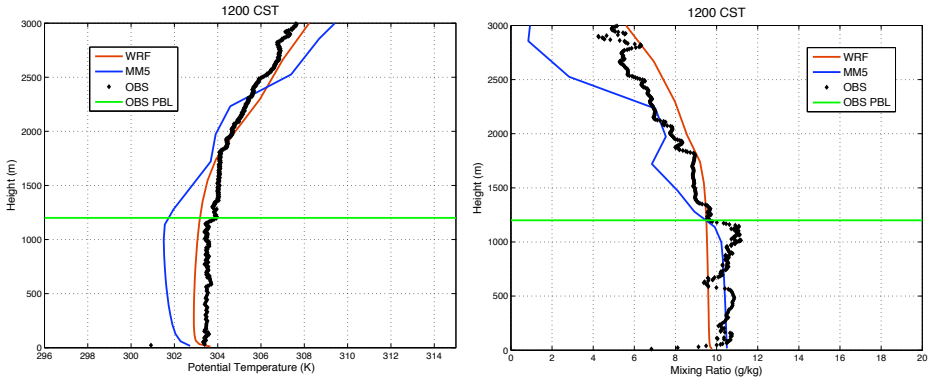

(c)

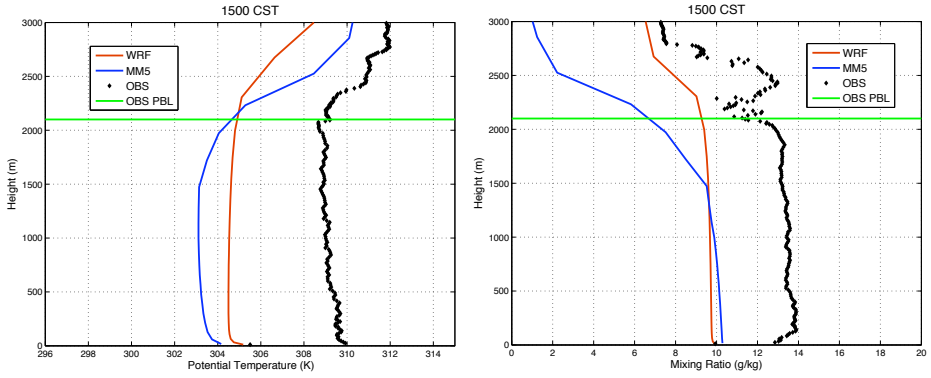

(d)

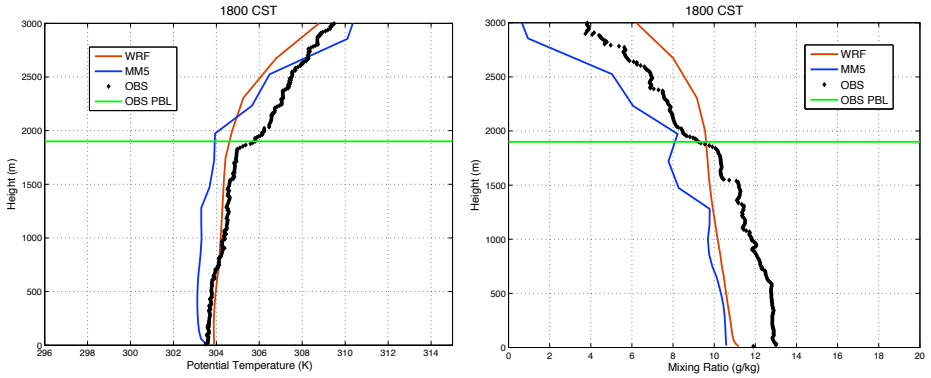

(e)

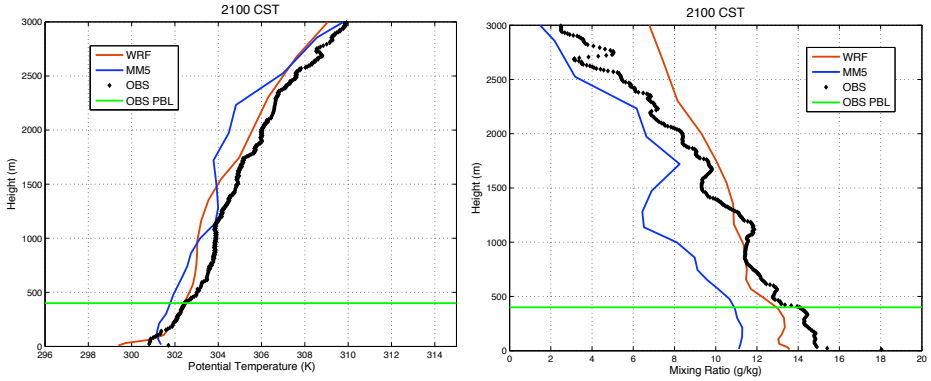

Figure 3.7: Vertical profiles of potential temperature (left) and mixing ratio (right) as recorded from radiosonde balloons launched at Moody Tower, TX on September 7, 2006 at (a) 0900, (b) 1200, (c) 1500, (d) 1800, and (e) 2100 CST.

At 0900 CST (Figure 3.7a), vertical profiles predicted by WRF-ACM2 and MM5-Eta shows realistic PBL heights, although both meteorological models under-predicted moisture at the surface. At 1200 CST (Figure 3.7b), MM5-Eta profiles closely match observations with a 1200 m deep PBL, while the WRF-ACM2 profile indicates a PBL height that is about 1700 meters deep, approximately 100 meters higher than the PBL height output by WRF at 1200 CST, shown in Figure 3.6. The WRF-ACM2 profile much more closely matched observations at 1500 CST (Figure 3.7c) with a PBL height of about 2300 m, although the actual WRF output PBL for 1500 CST was about 300 m higher (Figure 3.6). The vertical profile for MM5-Eta at 1500 CST indicates

a shallower PBL height of about 1500m, and WRF and MM5 under-predicted both surface temperature and moisture. Figure 3.7d shows the vertical profiles at 1800 CST, with the MM5-Eta model under-predicting the PBL height by about 600m, although the actual output PBL by MM5 (Figure 3.6) was 500 m even more shallow than that predicted by the profile, at a height of only 800 m. The WRF-ACM2 profile indicates a PBL height of 2300 m at 1800 CST, compared to the radiosonde observed PBL of about 1900 m, with the actual WRF output PBL being about 2500 m. The 400 m PBL height diagnosed from the observed vertical profile at 2100 CST (Figure 3.7e) was not predicted by either model or observed by the lidar backscatter profile (Figure 3.6), but both modeled profiles indicate an extremely shallow, post-evening-collapse PBL.

Chapter 4

Discussion

The recently developed ACM2 PBL scheme was evaluated for use in regulatory air quality models in eastern Texas using a spatially and temporally diverse observational dataset collected during the TexAQS II and TRAMP field campaigns between August and October of 2006. Outputs from WRF V3.1 using the ACM2 PBL scheme were compared with these observations and with outputs from MM5 V3.7.3 using the Eta PBL scheme, the meteorological model currently being used to develop O_3 control strategies in the HGB area. Both models were given a rigorous test of their ability to predict realistic PBL heights during daytime convective conditions across varying terrains. Variables that affect PBL height as a result of each model's land-surface model were also investigated to determine biases that would not be the fault of each respective model's PBL scheme.

The spatially diverse set of RWP-derived PBL heights were used to compare both model's ability to predict accurate PBL heights at varying terrains and distances from the coast. WRF-ACM2 produced more accurate PBL heights than MM5-Eta at all ten RWP locations and at all periods of the day, with MM5-Eta having the most trouble predicting accurate daily peak and evening collapse PBL heights at the furthest inland sites. Time series plots revealed that MM5-Eta was drastically under-predicting afternoon peak PBL heights and collapsing the PBL height too early at all three regions

(Central Texas, Inland, Coastal Plains), whereas the WRF-ACM2 model was slightly over-predicting the afternoon peak at the Inland and Coastal Plains locations, but also collapsing the PBL more rapidly than observations for all three regions.

The RWP analysis reveals a major weakness in the MM5-Eta model's ability to accurately simulate PBL evolution during convective conditions, a commonly reported insufficiency of local closure PBL schemes. Alternatively, WRF-ACM2 predicted a much more accurate PBL evolution, both temporally and spatially, in Eastern Texas. Inspection of median surface temperature and moisture time series plots revealed higher surface temperatures in WRF with more surface moisture in MM5, although these could not be attributed to surface heat fluxes, and thus the differences in performance of the WRF and MM5 models are likely due to the PBL schemes.

Vertical profiles of temperature and moisture collected from radiosonde balloons on September 7, 2006 were used to evaluate the PBL schemes in the lowest 3 km of the atmosphere. WRF closely matched the rapidly rising PBL indicated by the lidar-derived PBL heights, while MM5 predicted a more slowly rising and shallow PBL not representative of the daytime urban boundary layer. WRF's close comparisons to radiosonde profiles at five times during the day during mostly clear, low wind conditions further validate ACM2's ability to accurately represent the PBL during daytime convective conditions.

Chapter 5

Conclusions

An accurate depiction of the diurnal evolution and vertical mixing within the PBL is necessary for realistic air quality simulations. For the current meteorological modeling in support of HGB O_3 attainment demonstration, TCEQ chose the Eta PBL scheme, a local closure TKE model shown in this study to be inadequate at representing the daytime convective boundary layer. Eastern Texas is characterized by a considerable spatial variability of PBL height due to its coastal location and variations in land use, and thus requires a PBL scheme that can more accurately represent this variability. The recently developed combined local and nonlocal closure ACM2 PBL scheme was shown here to accurately simulate the morning growth, maximum height, and evening decay of the daytime PBL across varying regions in eastern Texas, while producing realistic vertical profiles of temperature and moisture at Moody Tower in downtown Houston.

Bibliography

Banta, R., Seniff, C., Nielsen-Gammon, J., Darby, L., Ryerson, T., Alvarez, R., Sandberg, S., Williams, E., Trainer, M., 2005. A bad air day in houston. B Am Meteorol Soc 86, 657–669.

Blackadar, A. K., 1978. Modeling pollutant transfer during daytime convection. Preprints, Fourth Symposium on Atmospheric Turbulence, Diffusion, and Air Pollution, Reno, NV, Amer. Meteor. Soc., 443–447.

Brown, A. R., 1996. Evaluation of parameterization schemes for the convective boundary layer using large-eddy simulation results. Bound-Lay Meteorol 31, 167–200.

Byun, D. W., Pleim, J. E., Tang, R. T., Bourgeois, A., 1999. Meteorology-chemistry interface processor (mcip) for models-3 community multiscale air quality (cmaq) modeling system. Office of Research and Development, US Environmental Protection Agency, Research Triangle Park, NC.

Dabberdt, W. F., Carroll, M. A., Baumgardner, D., Carmichael, G., Cohen, R., Dye, T., Ellis, J., Grell, G., Grimmond, S., Hanna, S., Irwin, J., Lamb, B., Madronich, S., McQueen, J., Meagher, J., Odman, T., Pleim, J., Schmid, H. P., Westphal, D. L., 2004. Meteorological research needs for improved air quality forecasting: Report of the 11th prospectus development team of the u.s. weather research program. B Am Meteorol Soc 85, 563–586.

Darby, L., 2005. Cluster analysis of surface winds in houston, texas, and the impact of wind patterns on ozone. J Appl Meteorol 44, 1788–1806.

Ek, M. B., Mitchell, K. E., Lin, Y., Rogers, E., Grunmann, P., Koren, V., Gayno, G., Tarpley, J. D., 2003. Implementation of noah land surface model advances in the national centers for environmental prediction operational mesoscale eta model. J. Geophys. Res. 108.

Flynn, C. J., 2006. Tramp nocturnal mixing from micropulse lidar measurements (tnmpl) final report. TERC Project H-81.

Grell, G., Dudhia, J., Stauffer, D., for Atmospheric Research. Mesoscale, N. C., Dicision, M. M., 1994. A description of the fifth-generation penn state/ncar mesoscale model (mm5).

Hu, X.-M., Nielsen-Gammon, J. W., Zhang, F., Sep 2010. Evaluation of three planetary boundary layer schemes in the wrf model. J Appl Meteorol Clim 49 (9), 1831–1844.

Janjic, Z., 1990. The step-mountain coordinate: Physical package. Monthly Weather Review 118 (7), 1429–1443.

Janjic, Z., 1994. The step-mountain eta coordinate model: Further developments of the convection, viscous sublayer, and turbulence closure schemes. Mon Wea Rev 122, 927–945.

Kain, J., Jan 2004. The kain-fritsch convective parameterization: An update. Journal of Applied Meteorology 43 (1), 170–181.

Knoderer, C. A., MacDonald, C. P., Aug 2007. Texaqs-ii radar wind profiler, radio acoustic sounding system, sodar, and lidar data quality control and mixing height derivation, 1–22.

Ku, J., Mao, H., Zhang, K., Civerolo, K., Rao, S., Philbrick, C., Doddridge, B., Clark, R., 2001. Numerical investigation of the effects of boundary-layer evolution on the predictions of ozone and the efficacy of emission control options in the northeastern united states. Environ Fluid Mech 1 (2), 209–233.

Lefer, B., Rappenglück, B., 2010. The texaqs-ii radical and aerosol measurement project (tramp). Atmos Environ 44 (33), 3997–4004.

Mlawer, E., Taubman, S., Brown, P., Iacono, M., Clough, S., 1997. Radiative transfer for inhomogeneous atmospheres: Rrtm, a validated correlated-k model for the longwave. J. Geophys. Res. 102, 16663–16682.

Morrison, H., Gettelman, A., 2008. A new two-moment bulk stratiform cloud microphysics scheme in the community atmosphere model, version 3 (cam3). part i: Description and numerical tests. Journal of Climate 21 (15), 3642–3659.

Nielsen-Gammon, J., Tobin, J., Bliujus, S., Myoung, B., McRoberts, B., 2008a. Terc project h84: Development of databases and charaterization of meteorological conditions for the texaqs ii intensive period, 1–55.

Nielsen-Gammon, J. W., Powell, C. L., Mahoney, M. J., Angevine, W. M., Senff, C., White, A., Berkowitz, C., Doran, C., Knupp, K., 2008b. Multisensor estimation of mixing heights over a coastal city. J Appl Meteorol Clim 47 (1), 27–43.

Otte, T., Pleim, J., 2010. The meteorology-chemistry interface processor (mcip) for the cmaq modeling system: updates through mcipv3.4.1. Geoscientific Model Development 3, 243–256.

Parrish, D. D., Allen, D. T., Bates, T. S., Estes, M., Fehsenfeld, F. C., Feingold, G., Ferrare, R., Hardesty, R. M., Meagher, J. F., Nielsen-Gammon, J. W., Pierce, R. B., Ryerson, T. B., Seinfeld, J. H., Williams, E. J., 2009. Overview of the second texas air quality study (texaqs ii) and the gulf of mexico atmospheric composition and climate study (gomaccs). J. Geophys. Res. 114.

Pérez, C., Jiménez, P., Jorba, O., Sicard, M., 2006. ... the pbl scheme on high-resolution photochemical simulations in an urban coastal area over .... Atmos Environ 40 (27), 5274–5297.

Pleim, J., 2006. A simple, efficient solution of flux-profile relationships in the atmospheric surface layer. J Appl Meteorol Clim 45 (2), 341–347.

Pleim, J., 2007a. A combined local and nonlocal closure model for the atmospheric boundary layer. part i: Model description and testing. J Appl Meteorol Clim 46 (9), 1383–1395.

Pleim, J., 2007b. A combined local and nonlocal closure model for the atmospheric boundary layer. part ii: Application and evaluation in a mesoscale meteorological model. J Appl Meteorol Clim 46 (9), 1396–1409.

Pleim, J., Chang, J., 1992. A non-local closure model for vertical mixing in the convective boundary layer. Atmos Environ. Part A. General Topics 26 (6), 965–981.

Rappenglück, B., Perna, R., Zhong, S., Morris, G. A., 2008. An analysis of the vertical structure of the atmosphere and the upper-level meteorology and their impact on surface ozone levels in houston, texas. J. Geophys. Res. 113.

Seaman, N., 2000. Meteorological modeling for air-quality assessments. Atmos Environ 34 (12-14), 2231–2259.

Skamarock, W. C., Klemp, J. B., Dudhia, J., Gill, D. O., Barker, D. M., Duda, M., Huang, H., Wang, W., Powers, J. G., 2008. A description of the advanced research wrf version 3, 1–125.

TCEQ, Mar 2010. Revisions to the state implementation plan for the control of ozone air pollution, houston-galveston-brazoria 1997 eight-hour ozone standard nonattainment area, 1–152.
URL `http://www.tceq.texas.gov/implementation/air/sip/HGB_eight_hour.html`

Vizuete, W., Jeffries, H., Christoph, E., 2008. Harc project h87 (unc) multi-resolution simulation and analysis of texaqs ii air .... files.harc.edu.

Wilczak, J. M., Djalalova, I., McKeen, S., Bianco, L., Bao, J.-W., Grell, G., Peckham, S., Mathur, R., McQueen, J., Lee, P., 2009. Analysis of regional meteorology and surface ozone during the texaqs ii field program and an evaluation of the nmm-cmaq and wrf-chem air quality models. J of Geophys Res-Atmos 114, D00F14.

Xiu, A., Pleim, J., 2001. Development of a land surface model. part i: Application in a mesoscale meteorological model. Journal of Applied Meteorology 40 (2), 192–209.

Zhang, F., Bei, N., Nielsen-Gammon, J., Li, G., Zhang, R., Stuart, A., Aksoy, A., 2007. Impacts of meteorological uncertainties on ozone pollution predictability estimated through meteorological and photochemical ensemble forecasts. J. Geophys. Res 112.